Optical Birefringence Fiber Temperature Sensors in the Visible Spectrum of Light

Martin KYSELAK[1], *Filip DVORAK*[2], *Jan MASCHKE*[1], *Cestmir VLCEK*[1]

[1]Department of Electrical Engineering, Faculty of Military Technology,
University of Defense, Kounicova 65, 662 10 Brno, Czech Republic
[2]Department of Radar Technology, Faculty of Military Technology,
University of Defense, Kounicova 65, 662 10 Brno, Czech Republic

martin.kyselak@unob.cz, filip.dvorak@unob.cz, jan.maschke@email.cz, cestmir.vlcek@unob.cz

DOI: 10.15598/aeee.v15i5.2419

Abstract. *This article describes experimental tests to determine PM fibers Panda style responses to a thermal source with different initial temperature. The aim of this study was to determine the sensitivity of a polarization maintaining fiber to the radiating heat, and to upgrade the space configuration and time response when using the 635 nm light. The sensitivity of the polarization maintaining fiber during excitation of both polarization modes is the principle of this sensor function. This excitation is caused by temperature change and by absorption of thermal radiation. This mechanism is used as an indicator for detection of temperature field disturbance. This article also provides links to previously published results and compares them to the results in this article.*

Keywords

Birefringence, fiber sensor, optical fiber polarization maintaining, phase shift, PMF, stokes vector, temperature field disturbance.

1. Introduction

Polarization Maintaining Fibers (PMF) work on the basis of creating mechanical strain that causes artificial birefringence. Typical fiber applications include cases, where state polarization maintenance along the light propagation through the fiber is required, and where the excitation of one polarization axis occurs. One effective way of creating birefringence is arranging structures with different thermal expansion into a fiber cladding. At an excitation of both polarization axes, when the light propagates through the fiber, the phase shift occurs between these axes. The measurement site and set of measurement results were published in [1] and [2]. Comparison works describing highly birefringence fibers, temperatures and strains, measurements, dependences and other new generation of optical fiber sensors are described in [3] and [4].

The phase shift is dependent on temperature and therefore also on incident thermal radiation. This phase shift can be evaluated by polarizer. Previous experiments [1] and [2] showed that the most suitable fiber, from the sensitivity point of view, is PANDA type fiber. The achieved results suggest to apply such sensor in cases, where the temperature field was disturbed by human body proximity, i.e. in the range of specific temperatures. This paper deals with the same site and arrangement as the previous experiments, but components for wavelength of 635 nm were used.

Suitable application could be, for example, for property protection against illegal manipulation, and thus, some requirements for the sensor sensitivity, system configuration and time response were established. The aim of this article is to analyze the influence of polarization angle setup on the input and output polarizer. And finally, to examine this problem in spread range temperature too.

2. Model of Fiber Thermal Segment Exposition

A thermal source was simulated by a plastic basin with various water temperatures. This arrangement enabled changes to the test water temperature, to the distance from basin bottom to the fiber and also to the number of exposed fiber segments. An ideal model of

$$\begin{bmatrix} E_x \\ E_y \end{bmatrix} = \begin{bmatrix} \cos^2\theta & \cos\theta\cdot\sin\theta \\ \cos\theta\cdot\sin\theta & \sin^2\theta \end{bmatrix} \cdot \frac{1}{2} \cdot \begin{bmatrix} e^{i\delta+1} & e^{i\delta-1} \\ e^{i\delta-1} & e^{i\delta+1} \end{bmatrix} \cdot \begin{bmatrix} \cos\beta \\ \sin\beta \end{bmatrix} = \\ = \frac{1}{2} \cdot \begin{bmatrix} \cos^2\theta & \cos\theta\cdot\sin\theta \\ \cos\theta\cdot\sin\theta & \sin^2\theta \end{bmatrix} \cdot \begin{bmatrix} e^{i\delta}(\cos\beta+\sin\beta)+(\cos\beta-\sin\beta) \\ e^{i\delta}(\cos\beta+\sin\beta)-(\cos\beta-\sin\beta) \end{bmatrix}. \quad (1)$$

a fiber sensor, for detection of temperature field disturbance caused by various water temperature in the basin, was set to simulate realistic conditions and also to define analysis and subsequent conditions. Thermal exposition was performed by defined temperature of water with the basin bottom placed 6 cm from the exposed fiber segment. For shorter distances (up to 1 cm), the response of PMF had linear characteristic, and for longer distances, it had non-linear characteristic [2]. Water temperature of 0 °C and 53 °C was used. For a comparison, a reference measurement for 35 °C (Approx. human body temperature) was made. The following mechanisms needed to be considered for temperature transfer to the fiber: thermal radiation of the basin, conduction heat transfer and convection.

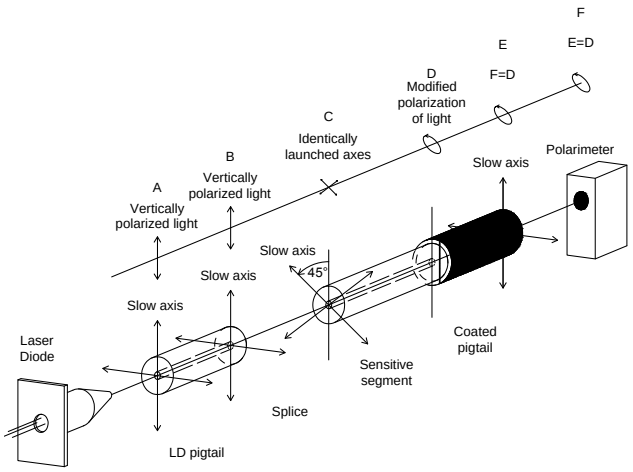

Fig. 1: Floor projection of measuring workplace with exposed length depiction and its sectional view.

For maximum response of the sensor element, it was necessary to excite both polarization axes uniformly. This could be achieved by circular polarization excitation or by the axes excitation caused by linear polarization angle of $\pi/4$. The advantage of the first solution is that the polarization axes of the fiber might have an orientation relative to the rotation; the disadvantage is the need to include a phase retarder of $\pi/4$ behind the LD output with an expected linear polarization character. Preferably, the second solution introduces the optical power of the laser diode directly into the fiber. However, the disadvantage is the need of the exact orientation of the optical fiber axes relative to the laser polarization. Given that the sensor should form a compact unit, the second variant seems advantageous, where the mutual rotation of the input linear polarization towards the polarization axes can be achieved by appropriate orientation of the connector and optical fiber. The system can be described as Jones vectors and matrixes (Eq. (1)) [7], [8] and [9]. Where β is the angle between input linear polarization and axis x, θ is the angle between axis of linear polarizer and axis x, δ is the phase shift between the polarization axes.

The coherent matrix behind the optical fiber (before the polarizer) is:

$$J_L = \frac{1}{2}\begin{bmatrix} 1+\cos 2\beta\cos\delta & \sin 2\beta-\cos 2\beta\sin\delta \\ \sin 2\beta+\cos 2\beta\sin\delta & 1-\cos 2\beta\cos\delta \end{bmatrix}. \quad (2)$$

The values of Stokes parameters are:

$$\begin{aligned} S_1 &= \cos 2\beta\cos\delta, \\ S_2 &= \sin 2\beta, \\ S_3 &= \cos 2\beta\sin\delta. \end{aligned} \quad (3)$$

When the fiber rotation is exactly set at $\pi/4$ and the angle of input intensity $\beta = 0$, Stokes parameters are $\cos\delta$, 0, $\sin\delta$. Responses to the arrangement of optical fiber polarimeter are shown in [9].

The resulting intensity of the optical wave output was:

$$I = \frac{1}{2}\cdot(1+\sin 2\theta\sin 2\beta+\cos 2\theta\cos 2\beta\cos\delta). \quad (4)$$

By substituting numerical values, it can be shown that in the range of reasonable error settings, approximately ±5°, the deviation of the mean value was approximately 3 %. In terms of the evaluation phase, it was not substantial [7], [8] and [9].

3. Mechanism of Heat Transfer

Transferred heat Q_T from water of temperature T_e to a fiber of temperature T was calculated as follows [6]:

$$Q_T = \lambda_T\frac{S}{\Delta l}(\Delta T_e-\Delta T)t = K_T(\Delta T_e-\Delta T)t, \quad (5)$$

where λ_T is a coefficient of thermal conductivity, Δl is the heat source (basin bottom) distance from the fiber segment, S is the surface area, ΔT_e is temperature difference between the source and ambient temperature, ΔT is the temperature difference between the

water and ambient temperature and t is time. As the phase shift was calculated with respect to the change of temperature, all the temperatures were relative to the initial temperature of the fiber, i.e. to the difference between the given and the ambient temperature.

As the transfer of heat depended on the difference between the temperatures, we substituted the difference of absolute temperatures T by the difference of temperatures $\Delta\vartheta$ in °C, in which the temperature of the applied water was measured. The following formula was obtained:

$$Q_T = K_T(\Delta\vartheta_e - \Delta\vartheta)t. \tag{6}$$

4. Experimental Results

Firstly, we prepared the measurement equipment as a preliminary workplace. We took advantage of the benefits of our new polarimeter equipment. We could comfortably observe online the following: the development of SOP changes at outputs from the light source, linear in-fiber polarizer and PM fiber sensor. In this phase, we dismounted the linear polarizer on output and the photodiode, too. Then it was possible to observe the immediate polarization state on polarimeter. Our measured values are the demonstration of functionality of our temperature sensor (Fig. 2).

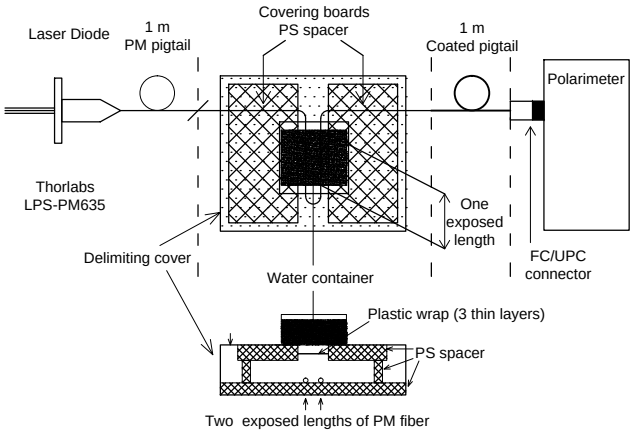

Fig. 2: The arrangement of fiber sensor model. Disposed optical fiber sensor was on the surface of the polystyrene plate. Cork stoppers were used as spacers. Measuring station was inclosed by polystyrene plates. The entire workstation was wrapped in polyethylene foam to avoid external thermal influences. Sensory fibers were accessible by upper slot for heat only.

The measurement workplace arrangement: Temperature controller TED200C, power current supply LDC202C - mounting TCLDM9 - optical source Thorlabs LPS-PM635-FC pigtail LD - connector FC/FC (ADAFC3) - fiber sensor = PM 635 fiber (length = 2 m, Lightcom/Safibra) - connector FC/FC (ADAFC3) - PM patch cord (PMJP-FC-FC-635-900-5-1) - Polarimeter PAX5720IR1-T.

5. Experimental Evaluation of the Time Response

Exciting two lengths (25 cm per length) of fiber 6 cm from heat source (basin of water), temperature at the time of attaching was 35 °C (human body), 0 °C and 53 °C. Heat source was located at time 2:20 min and removed at 7:50 min.

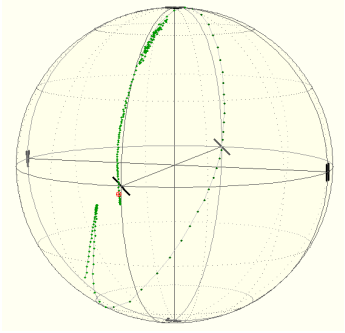

Fig. 3: One part of the ray on the Poincaré sphere (approximately 10 s), Thorlabs Polarimeter PAX5720IR1-T.

Total time was 920 s, ambient room temperature was 25 °C. Operating current source was 27.16 mA. The distance of heat source and sensor fiber was 6 cm. Measured by polarimeter Thorlabs PAX 5710.

Tab. 1: Measured polarization efficiency for PMF 2 m of length, excited by LD 635, exposition temperatures 35 °C, 0 °C and 53 °C.

Optical source	LPS-PM635-FC
Basic Sample Rate (SPS)	66.70
Signal Averaging	2
Result Averaging	3
Sample Time	0.18 s
Number of Measurements	1024
Record Rate	5

A demonstration of the time response for this set of components is depicted in Fig. 3 and Fig. 4. Firstly, (Fig. 3) shows the on-line exhibition from the polarimeter. We can see clearly one part of the ray on the Poincare sphere (approximately 10 s). Some difference in the output polarization is evident from this graph. From the viewpoint of clearness, the most important is Fig. 3, as it shows long periods, approximately 15 minutes. It represents the measurement for 0 °C. Thanks to the reference (25 °C) measurement, this can be considered authoritative. A demonstration of the time response for this set of components is depicted in Fig. 3 and Fig. 4. Firstly, (Fig. 3) shows the on-line exhibition from the polarimeter. We can see clearly one

part of the ray on the Poincaré sphere (approximately 10 s). Some difference in the output polarization is evident from this graph. From the viewpoint of clearness, the most important is Fig. 3, as it shows long periods, approximately 15 minutes. It represents the measurement for 0 °C. Thanks to the reference (25 °C) measurement, this can be considered authoritative.

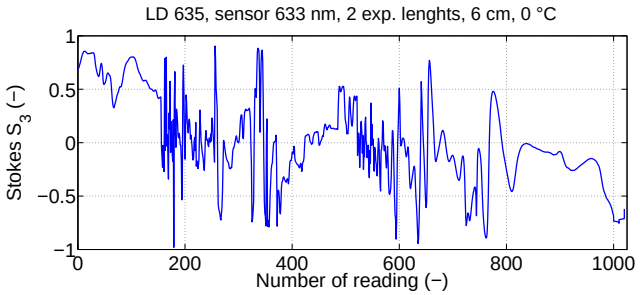

(a) Water temperature 0 °C

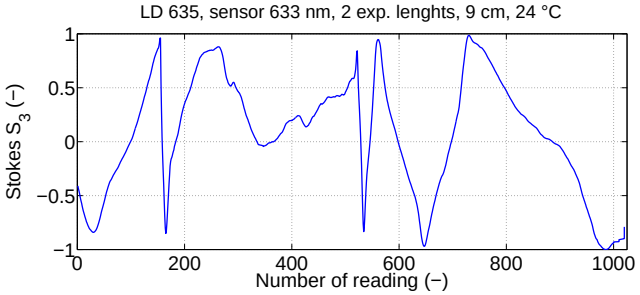

(b) Water temperature 24 °C

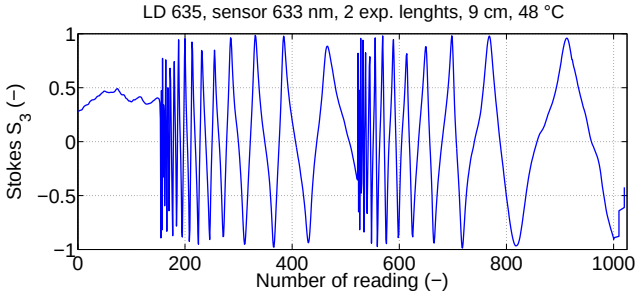

(c) Water temperature 48 °C

Fig. 4: The evolution of the output Stokes element S_3.

By comparing the results, the conclusion was different responses of PMF sensor to minus Δ and plus Δ temperature from human body temperature. This was caused by different mechanisms of the heat transfer. SOP development in polarization maintaining fiber sensor. The track of the light polarization state on the Poincare sphere was very similar in each deflection caused by temperature change. When the heat source was removed, the track in reverse direction was clearly observed.

By comparing with the previously published results [1] it seems that the response in the visible spectrum of light is more massive. It can be due to beat length, which is double for 635 nm.

As shown in Fig. 4, the temperatures influence is minimal when the measured medium temperature is approaching to ambient temperature. The delta of temperatures have to be the same response but it is not due to different heat transfer.

A typical progress on regular circle was unfortunately disturbed by some inaccuracies, inhomogeneity and reflections, especially on the connectors. The amplitude fluctuation was apparently caused by sampling. There were also some other affecting factors: imperfect excitement of both axes, low degree of coherence, but also a noncircular LD beam profile. From practical realization point of view, it is also necessary to take into considerations the excitation by LD, with regard to the compatibility of individual sensor components.

Tab. 2: The measurement process by Thorlabs Polarimeter PAX5720IR1-T.

ER Measurement Results	
Poits per measurement	300
Used Points	223
Extinction Ratio	0.87 dB
Center Azimuth	−2.64°
Radius	84.27°
Deviation	2.416°
Settings	
Wavelength	633.000 nm
Sample Rate	33.333 SPS
Measurement Time	10 s
Measurement	
Azimuth	−45.467°
Elipticity	−1.461°
Degree of Polarization	64.802 %
Power	2.422 dBm

6. Conclusion

The described temperature sensor at 635 nm can be used in many different ways. The above described arrangement, all component exactly as in-line fiber construction, can be used with advantages in many industrial sectors. This construction largely eliminates the sensitivity to other factors, e.g. mechanical vibration, radiation or pressure changes. For significant exposed length, there was an appropriate response. The option of adjusting sensitivity by changing the exposed length is also advantageous. A fast sensor response was achieved by simultaneous exposition of short segments. When compared to the previous measurement [1], we can clearly state that both wavelengths are suitable for this type of sensor. The degree of sensitivity will be the subject of further research.

Future work will be aimed at the studying of 1310 nm wavelength and comparing the results with previous

studies. The trend of development will be directed to replace the connector by splicing. Gradual replacement of polarimeter may allow to use linear in-line fiber polarizer and photodiode.

Acknowledgment

This work has been supported from the Program for the organization development of K217 and K207 Departments, Brno University of Defense. The research team would like to thank the company SQS Vlaknova optika a. s. for assistance in the production of special patch cords and assembly of fiber-optic components.

References

[1] KYSELAK, M., C. VLCEK, J. MASCHKE and F. DVORAK. Optical fibers with high birefringence as a sensor element. In: *6th International Conference on Electronics Information and Emergency Communication (ICEIEC)*. Beijing: IEEE, 2016, pp. 190–193. ISBN 978-1-5090-1997-7. DOI: 10.1109/ICEIEC.2016.7589717.

[2] DVORAK, F., J. MASCHKE and C. VLCEK. Utilization of birefringent fiber as sensor of temperature field disturbance. *Radioengineering*. 2009, vol. 18, iss. 4, pp. 639–643. ISSN 1210-2512.

[3] LESIAK, P., G. RAJAN, Y. SEMENOVA, G. FARRELL, A. BOCZKOWSKA, A. DOMANSKI and T. WOLINKSKI. A Hybrid Highly Birefringent Fiber Optic Sensing System for Simultaneous Strain and Temperature Measurement. *Photonics Letters of Poland*. 2010, vol. 2, iss. 3, pp. 140–142. ISSN 2080-2242. DOI: 10.1109/JSEN.2011.2114650.

[4] ERTMAN, S., P. LESIAK and T. R. WOLINSKI. Optofluidic Photonic Crystal Fiber-Based Sensors. *Journal of Lightwave Technology*. 2017, vol. 35, iss. 16, pp. 3399–3405. ISSN 1558-2213. DOI: 10.1109/JLT.2016.2596540.

[5] JIN, Y., C. C. CHAN., Y. ZHANG, X. DONG and P. ZU. Temperature sensor based on a pressure-induced birefringent single-mode fiber loop mirror. *Measurement Science and Technology*. 2010, vol. 21, no. 6, pp. 1–5. ISSN 0957-0233. DOI: 10.1088/0957-0233/21/6/065204.

[6] WALKER, J., D. HALLIDAY and R. RESNICK. *Fundamentals of Physics*. 10th ed. Hoboken: Wiley, 2014. ISBN 978-1-118-23072-5.

[7] COLLETT, E. and B. SCHAEFER. Visualization and calculation of polarized light. I. The polarization ellipse, the Poincare sphere and the hybrid polarization sphere. *Applied Optics*. 2008, vol. 47, no. 22, pp. 4009–4016. ISSN 2155-3165. DOI: 10.1364/AO.47.004009.

[8] BORN, M. and E. WOLF. *Principles of Optics*. 7th ed. Cambridge: Cambridge University Press, 1999. ISBN 978-0-521-64222-4.

[9] COLLETT, E. *Polarized Light in Fiber Optics*. 7th ed. New Jersey: SPIE, 2003. ISBN 978-0-819-45761-5.

About Authors

Martin KYSELAK was born in 1981. He is an assistant of the Department of Electrical Engineering. He graduated from Brno University of Technology, Faculty of electrical engineering and communication, field of Electronics and communication. He is engaged in studies covering increase of the transmission speed over optical fibers, using the multiplex. A part of his work is to suggest measures for lowering unfavorable effects, first of all chromatic and polarization dispersion, on signal transmission over optical fibers. He teaches in these courses: "Electrical Components".

Filip DVORAK was born in 1977. He received his M.Sc. degree from the Brno Military Academy in 2004 and Ph.D. degree in 2011. He is currently lecturer with the Department of Radar Technology, Brno University of Defense. His work is focused on the modelling of fibers and optical components by means of matrix methods in the MATLAB environment and analysis of fiber sensors.

Jan MASCHKE was born in 1942. He received his M.Sc. degree in 1965 and Ph.D. degree in 1978. He was a teacher at the Technical school at Liptovsky Mikulas and at the Military Academy since 1968, and associate professor of the Department of electrical engineering since 1985. He retired in 2005. His research work focused on the problems of fiber optics and fiber sensors.

Cestmir VLCEK was born in 1946. He received his M.Sc. degree in 1969 and Ph.D. degree in 1980. He was a teacher at the Military Academy since 1969, associate professor since 1985, head of the Electrical Engineering and Electronics Department since 1997 and professor since 2000. His research work during the last years was aimed at problems of optoelectronic signals and systems, single mode fiber components modelling, atmospheric optical communication systems and analysis of sensors for military applications.